arXiv:2503.14610v1 [hep-ph] 18 Mar 2025

Modular S_3 flavoured Pati-Salam model with two family seesaw

A. E. Cárcamo Hernández[a,b,c*]
[a] *Universidad Técnica Federico Santa María, Casilla 110-V, Valparaíso, Chile*
[b] *Centro Científico-Tecnológico de Valparaíso, Casilla 110-V, Valparaíso, Chile*
[c] *Millennium Institute for Subatomic Physics at the High-Energy Frontier, SAPHIR, Calle Fernández Concha No 700, Santiago, Chile*

Ivo de Medeiros Varzielas[†]
CFTP, Departamento de Física, Instituto Superior Técnico, Universidade de Lisboa, Avenida Rovisco Pais 1, 1049 Lisboa, Portugal

S. F. King[‡]
School of Physics and Astronomy, University of Southampton, SO17 1BJ Southampton, United Kingdom

Vishnudath K. N.[§]
Departamento de Física, Universidad Técnica Federico Santa María, Casilla 110-V, Valparaíso, Chile

(Dated: March 20, 2025)

We present a unified model of quarks and leptons with modular S_3 flavour symmetry, where the two lightest family masses are naturally suppressed via a Pati-Salam version of the type I seesaw mechanism, mediated through heavier vector-like fermions. Majorana neutrino masses are further suppressed through a double seesaw mechanism. The viable parameter space has a preferred range of the modulus field with $\mathrm{Im}(\tau) \sim 2$, leading to successful fermion masses and mixing. The prediction for neutrinoless double beta decay is partly within the reach of the nEXO experiment. In particular, the Dirac CP violating neutrino oscillation phase is predicted to lie in the range $\delta^{\nu}_{\mathrm{CP}} \sim 260^o - 360^o$.

I. INTRODUCTION

Despite its remarkable agreement with experimental data, the current theory of strong and electroweak interactions - the standard model (SM) of particle physics - lacks an underlying mechanism to explain the strong hierarchy in the masses of elementary charged fermions. Additionally, the different mixing patterns in the quark and lepton sectors remain unexplained within the SM. The theory also fails to account for several issues, such as the tiny masses of active neutrinos and the origin of parity violation in the electroweak interaction, whose basic V-A nature is introduced by hand in the formulation of the Standard Model. This has motivated the development of several new physics models that aim to explain some or all of these unresolved issues.

Recently, the use of modular symmetries in extensions of the SM as a way of explaining the observed pattern of SM fermion masses and mixing angles has received a lot of attention from the theoretical particle physics community. See,

*Electronic address: antonio.carcamo@usm.cl
†Electronic address: ivo.de@udo.edu
‡Electronic address: king@soton.ac.uk
§Electronic address: vishnudath.neelakand@usm.cl

for instance, [1–17]. Models based on discrete flavor symmetry, along with modular symmetry do not include flavon fields in the particle spectrum excepting the modulus τ, thus making the scalar sector of these theories more minimal than that of models not having modular symmetries. When the complex modulus τ acquires a non-vanishing vacuum expectation value (*vev*), the flavor symmetry is spontaneously broken. Theories with modular flavor symmetries do not require the implementation of a mechanism responsible for the vacuum alignment, they need instead a mechanism to determine the modulus τ, which however we shall not address here. However, in modular flavor models, the Yukawa couplings depend on the modular forms, which are holomorphic functions of τ [1], which may thus be determined phenomenologically. For example, such models have been proposed with Pati-Salam unification together with A_4 modular symmetry [15]. The lightness of the first two families is not fully addressed in many such approaches, and to remedy this the weighton mechanism has been proposed [18], together with other strategies [2]. Here we shall follow a different path, motivated by the type I seesaw mechanism [19–24], in order to explain the smallness of the first and second family masses.

In this paper, in order to address the SM fermion flavor puzzle and to provide dynamical origin of the parity violation of the electroweak interactions, we propose a minimal modular model based on the smallest quark-lepton unified symmetry, the Pati-Salam $SU(4)_C \times SU(2)_L \times SU(2)_R$ gauge group [25], and the smallest modular symmetry, S_3. The modular S_3 is perfect for implementing a two-family seesaw mechanism, since it admits doublet representations. The masses of the third family of SM charged fermion arise from renormalisable Yukawa interactions involving a colourless scalar bi-doublet as well as a bi-doublet scalar in the adjoint representation of $SU(4)_C$. The Dirac masses of the first and second families (including neutrinos) arise from a generalised version of the type I seesaw mechanism, but applied to both charged and neutral Dirac masses [26–30]. In our proposed model, the tiny active Majorana neutrino masses then arise from a double seesaw mechanism. The model is shown to describe all quark and lepton (including neutrino) masses and mixing angles, in terms of high energy mass scales, together with complex dimensionless Yukawa coefficients which are all of order unity, and a single complex modulus field τ with $\mathrm{Im}(\tau) \sim 2$.

In Section II we present the details of the model, followed by a numerical study of the input parameters leading to viable observables in Section III. Section IV sumarises our findings. A review of modular flavour symmetry can be found in Appendix A.

II. THE MODEL

We propose an extended Pati-Salam theory where the $SU(4)_C \times SU(2)_L \times SU(2)_R$ gauge symmetry is supplemented by an S_3 modular symmetry. The masses of the third-generation SM charged fermions arise from Yukawa interactions involving the scalar bi-doublets Φ and Σ, which transform as singlet and adjoint representations of $SU(4)_C$, respectively.

The field content is enlarged by the inclusion of heavy vector-like fermions and right-handed Majorana neutrinos, required for the implementation of the tree level two family seesaw mechanism that yields the masses of the first and second generation of SM charged fermions as well as the Double Seesaw mechanism that produces the tiny masses of the light active neutrinos. Specifically, we have vector-like fermions Ψ_n and Ψ_n^c $(n = 1, 2)$ transforming as $(\mathbf{4}, \mathbf{1}, \mathbf{2})$ and $(\overline{\mathbf{4}}, \mathbf{1}, \overline{\mathbf{2}})$, respectively, under the Pati-Salam group. The vector-like fermions Ψ_n and Ψ_n^c $(n = 1, 2)$ are the seesaw messengers which mix with the SM fermionic multiplet fields F_i and F_i^c $(i = 1, 2, 3)$, also transforming as $(\mathbf{4}, \mathbf{1}, \mathbf{2})$ and $(\overline{\mathbf{4}}, \mathbf{1}, \overline{\mathbf{2}})$, respectively, under the Pati-Salam group. Such mixings between SM fermions and the seesaw messengers occurs thanks to the Yukawa interactions involving the singlet scalar fields σ_n $(n = 1, 2)$ as well as the $SU(4)_C$ adjoint scalars Ξ_1 and Ξ_2. Besides that, we include three Majorana neutrinos, S_i $(i = 1, 2, 3)$, which are singlets under the $SU(4)_C \otimes SU(2)_L \otimes SU(2)_R$ group, in order to implement the double seesaw mechanism for the generation of light active neutrino masses. The full symmetry $\mathcal{G}$ of our model features the following spontaneous breaking pattern:

	$SU(4)_C$	$SU(2)_L$	$SU(2)_R$	S_3	k
$F=(F_1,F_2)$	$\mathbf{4}$	$\mathbf{2}$	$\mathbf{1}$	$\mathbf{2}$	0
F_3	$\mathbf{4}$	$\mathbf{2}$	$\mathbf{1}$	$\mathbf{1'}$	-1
F_1^c	$\overline{\mathbf{4}}$	$\mathbf{1}$	$\overline{\mathbf{2}}$	$\mathbf{1}$	1
F_2^c	$\overline{\mathbf{4}}$	$\mathbf{1}$	$\overline{\mathbf{2}}$	$\mathbf{1'}$	-1
F_3^c	$\overline{\mathbf{4}}$	$\mathbf{1}$	$\overline{\mathbf{2}}$	$\mathbf{1'}$	1
Ψ_1	$\mathbf{4}$	$\mathbf{1}$	$\mathbf{2}$	$\mathbf{1'}$	-2
Ψ_2	$\mathbf{4}$	$\mathbf{1}$	$\mathbf{2}$	$\mathbf{1'}$	-4
Ψ_1^c	$\overline{\mathbf{4}}$	$\mathbf{1}$	$\overline{\mathbf{2}}$	$\mathbf{1'}$	2
Ψ_2^c	$\overline{\mathbf{4}}$	$\mathbf{1}$	$\overline{\mathbf{2}}$	$\mathbf{1'}$	4
$S^c=(S_1^c,S_2^c)$	$\mathbf{1}$	$\mathbf{1}$	$\mathbf{1}$	$\mathbf{2}$	1
S_3^c	$\mathbf{1}$	$\mathbf{1}$	$\mathbf{1}$	$\mathbf{1'}$	1
Φ	$\mathbf{1}$	$\mathbf{2}$	$\mathbf{2}$	$\mathbf{1}$	0
χ_R	$\overline{\mathbf{4}}$	$\mathbf{1}$	$\mathbf{2}$	$\mathbf{1}$	2
Σ	$\mathbf{15}$	$\mathbf{2}$	$\mathbf{2}$	$\mathbf{1}$	0
σ_1	$\mathbf{1}$	$\mathbf{1}$	$\mathbf{1}$	$\mathbf{1}$	7
σ_2	$\mathbf{1}$	$\mathbf{1}$	$\mathbf{1}$	$\mathbf{1}$	5
Ξ_1	$\mathbf{15}$	$\mathbf{1}$	$\mathbf{1}$	$\mathbf{1}$	7
Ξ_2	$\mathbf{15}$	$\mathbf{1}$	$\mathbf{1}$	$\mathbf{1}$	5
$Y_{\mathbf{1}}^{(4)}(\tau)$	$\mathbf{1}$	$\mathbf{1}$	$\mathbf{1}$	$\mathbf{1}$	4
$Y_{\mathbf{1}}^{(6)}(\tau)$	$\mathbf{1}$	$\mathbf{1}$	$\mathbf{1}$	$\mathbf{1}$	6
$Y_{\mathbf{2}}^{(2)}(\tau)$	$\mathbf{1}$	$\mathbf{1}$	$\mathbf{1}$	$\mathbf{2}$	2
$Y_{\mathbf{2}}^{(4)}(\tau)$	$\mathbf{1}$	$\mathbf{1}$	$\mathbf{1}$	$\mathbf{2}$	4
$Y_{\mathbf{2}}^{(6)}(\tau)$	$\mathbf{1}$	$\mathbf{1}$	$\mathbf{1}$	$\mathbf{2}$	6

Table I: The transformation properties of the scalar and fermionic fields, as well as those of the Yukawa couplings, under the Pati-Salam gauge group and S_3 modular symmetry, where the modular weights of the fields are labelled by k.

$$\begin{gathered}\mathcal{G}=SU(4)_C\otimes SU(2)_L\otimes SU(2)_R\otimes S_3\\ \Downarrow\Lambda_{PS}\\ SU(3)_C\otimes SU(2)_L\otimes SU(2)_R\otimes U(1)_{B-L}\\ \Downarrow v_R\\ SU(3)_C\otimes SU(2)_L\otimes U(1)_Y\\ \Downarrow v\\ SU(3)_C\otimes U(1)_Q\end{gathered}\tag{1}$$

where $v=246$ GeV and it is assumed that the Pati-Salam gauge symmetry is broken at the scale $\Lambda_{PS}\gtrsim 10^6$ GeV, which arises from the experimental bound on the branching ratio for the rare meson decays $K_L^0\to\mu^\pm e^\mp$ mediated by the vector leptoquarks, as indicated in Refs. [31, 32]. The $SU(4)_C\times SU(2)_L\times SU(2)_R$ Pati-Salam symmetry is spontaneously broken down to the $SU(3)_C\otimes SU(2)_L\otimes SU(2)_R\otimes U(1)_{B-L}$ gauge group by the *vevs* of the scalar multiplets Ξ_1 and Ξ_2 which transform as the adjoint representation of the Pati-Salam gauge group. The second stage of symmetry breaking is triggered by the *vev* of the scalar multiplet χ_R that transforms as a $(\overline{\mathbf{4}},\mathbf{1},\mathbf{2})$ under the

Pati-Salam group. The scalars χ_R, Φ and Σ develop *vevs* of the form

$$\langle\chi_R\rangle = \frac{1}{\sqrt{2}}\begin{pmatrix} 0 & 0 & 0 & v_R \\ 0 & 0 & 0 & 0 \end{pmatrix}, \qquad \langle\Phi\rangle = \frac{1}{\sqrt{2}}\begin{pmatrix} v_1 & 0 \\ 0 & v_2 \end{pmatrix}, \qquad \langle\Sigma\rangle = \frac{1}{\sqrt{2}}\begin{pmatrix} v_{\Sigma_1}T^{15} & 0_{4\times 4} \\ 0_{4\times 4} & v_{\Sigma_2}T^{15} \end{pmatrix}, \tag{2}$$

with $T^{15} = \frac{1}{2\sqrt{6}}\mathrm{diag}\,(1,1,1,-3)$.

The SM fermions can be written in component form as follows:

$$F_i = \begin{pmatrix} u_i & u_i & u_i & \nu_i \\ d_i & d_i & d_i & l_i \end{pmatrix}^T, \qquad F_i^c = \begin{pmatrix} u_i^c & u_i^c & u_i^c & \nu_i^c \\ d_i^c & d_i^c & d_i^c & l_i^c \end{pmatrix}, \qquad i = 1,2,3. \tag{3}$$

Similarly, the heavy vector-like fermionic multiplets Ψ_n and Ψ_n^c $(n = 1,2)$ containing the two family seesaw messengers are expressed as follows:

$$\Psi_n = \begin{pmatrix} U_n & U_n & U_n & N_n \\ D_n & D_n & D_n & E_n \end{pmatrix}^T, \qquad \Psi_n^c = \begin{pmatrix} U_n^c & U_n^c & U_n^c & N_n^c \\ D_n^c & D_n^c & D_n^c & E_n^c \end{pmatrix}, \qquad n = 1,2. \tag{4}$$

The transformation properties of the scalar and fermionic fields, as well as those of the Yukawa couplings, under the Pati-Salam gauge group and S_3 modular symmetry are given in Table-I. With this particle content and symmetries, the Yukawa superpotential compatible with the S_3 modular symmetry is:

$$\begin{aligned} -\mathcal{W} \;=\; & y_1 Y_{\mathbf{2}}^{(2)}(\tau)\, F\Phi\Psi_1^c + y_2 Y_{\mathbf{2}}^{(4)}(\tau)\, F\Phi\Psi_2^c + y_3 F_3\Phi F_3^c \\ & + z_1 Y_{\mathbf{1'}}^{(6)}\Psi_1\sigma_1 F_1^c + z_2 Y_{\mathbf{1}}^{(4)}(\tau)\,\Psi_1\sigma_1 F_2^c + z_3 Y_{\mathbf{1}}^{(4)}(\tau)\,\Psi_1\sigma_2 F_3^c + z_4\Psi_2\sigma_2 F_2^c + z_5 Y_{\mathbf{1}}^{(4)}(\tau)\,\Psi_2\sigma_1 F_3^c \\ & + w_1 Y_{\mathbf{1'}}^{(6)}\Psi_1\Xi_1 F_1^c + w_2 Y_{\mathbf{1}}^{(4)}(\tau)\,\Psi_1\Xi_1 F_2^c + w_3 Y_{\mathbf{1}}^{(4)}(\tau)\,\Psi_1\Xi_2 F_3^c + w_4\Psi_2\Xi_2 F_2^c + w_5 Y_{\mathbf{1}}^{(4)}(\tau)\,\Psi_2\Xi_1 F_3^c \\ & + x_1 Y_{\mathbf{2}}^{(2)}(\tau)\, F\Sigma\Psi_1^c + x_2 Y_{\mathbf{2}}^{(4)}(\tau)\, F\Sigma\Psi_2^c + x_3 F_3\Sigma F_3^c + m_{\Psi_1}\Psi_1\Psi_1^c + m_{\Psi_2}\Psi_2\Psi_2^c \\ & + \gamma_1 Y_{\mathbf{2}}^{(4)}(\tau)\, F_1^c\chi_R S^c + \gamma_2 Y_{\mathbf{2}}^{(2)}(\tau)\, F_2^c\chi_R S^c + \gamma_3 Y_{\mathbf{2}}^{(4)}(\tau)\, F_3^c\chi_R S^c \\ & + \gamma_4 Y_{\mathbf{1}}^{(4)}(\tau)\, F_3^c\chi_R S_3^c + M_1 Y_{\mathbf{2}}^{(2)}(\tau)\,(S^c S^c)_{\mathbf{2}} + M_2 Y_{\mathbf{2}}^{(2)}(\tau)\,(S^c S_3^c) + \text{h.c.}. \end{aligned} \tag{5}$$

The flavour structure of the superpotential is replicated with Φ, Σ having the same S_3 assignments (being distinguished by the gauge group), and the same holds for the pairs σ_1, Ξ_1 and for σ_2, Ξ_2. The two pairs are distinct as σ_1, Ξ_1 have modular weight $k = 5$ whereas σ_2, Ξ_2 have modular weight $k = 7$. This structure is also visible in the diagrams in Fig.1. The structure of the diagrams is similar to the diagram of the seesaw mechanism. In particular, the first two families of all the charged fermions obtain their masses via seesaw mechanism mediated by the heavy vector-like fermions Ψ_1 and Ψ_2, whereas the third families obtain their masses via their Yukawa couplings to Φ and Σ. The neutrinos also obtain Dirac masses in a similar way, which is further extended to Double Seesaw by the inclusion of the singlet fields S_i^c.

Due to the difference in modular weights, the superpotential terms are such that the effective Yukawa terms arise with the respective modular forms, leading to the following mass terms for charged fermions and neutrinos:

$$\begin{pmatrix} u_i & U_k \end{pmatrix}\begin{pmatrix} M_c^{(u)} & M_a^{(u)} \\ M_b^{(u)} & M_U \end{pmatrix}\begin{pmatrix} u_j^c \\ U_k^c \end{pmatrix}, \qquad \begin{pmatrix} d_i & D_k \end{pmatrix}\begin{pmatrix} M_c^{(d)} & M_a^{(d)} \\ M_b^{(d)} & M_D \end{pmatrix}\begin{pmatrix} d_j^c \\ D_k^c \end{pmatrix}, \tag{6}$$

$$\begin{pmatrix} e_i & E_k \end{pmatrix}\begin{pmatrix} M_c^{(e)} & M_a^{(e)} \\ M_b^{(e)} & M_E \end{pmatrix}\begin{pmatrix} e_j^c \\ E_k^c \end{pmatrix}, \qquad \begin{pmatrix} \nu_i & N_k \end{pmatrix}\begin{pmatrix} M_c^{(\nu)} & M_a^{(\nu)} \\ M_b^{(\nu)} & M_N \end{pmatrix}\begin{pmatrix} \nu_j^c \\ N_k^c \end{pmatrix}, \tag{7}$$

where the heavy vector-like seesaw mediator mass matrices are,

$$M_U = M_D = M_E = M_N = \begin{pmatrix} m_{\Psi_1} & 0 \\ 0 & m_{\Psi_2} \end{pmatrix}. \tag{8}$$

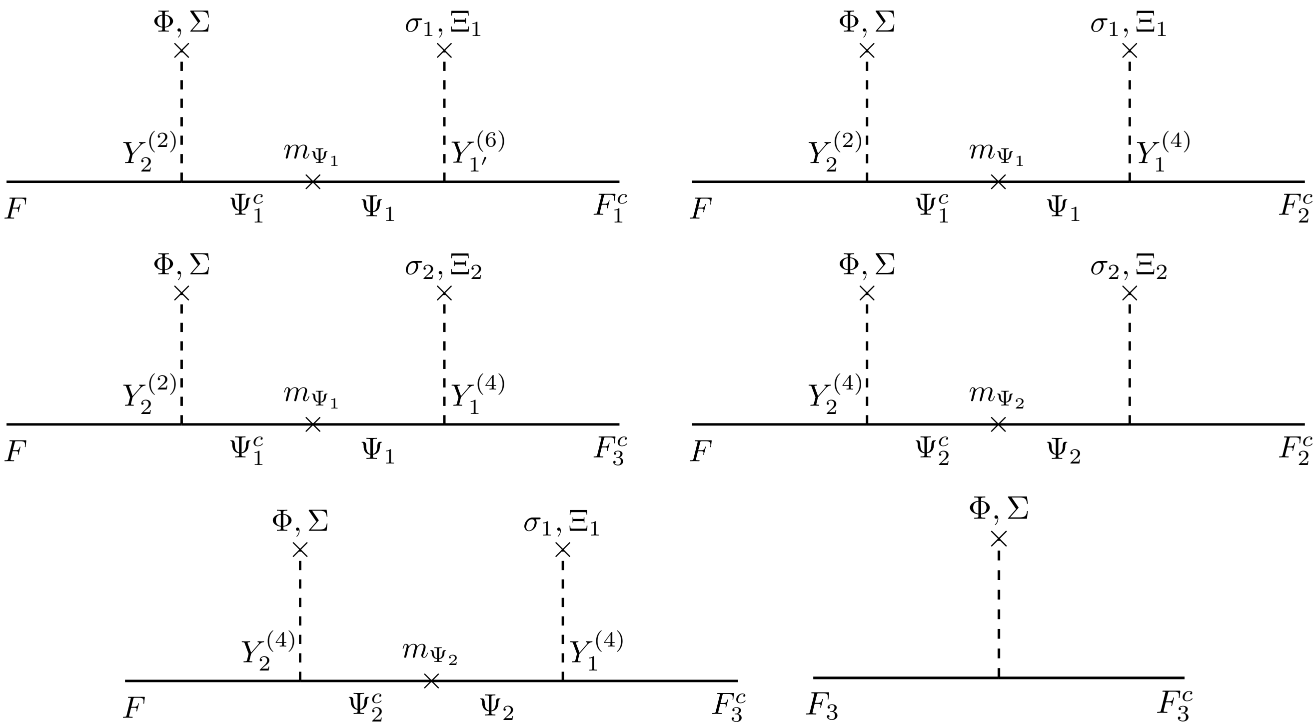

Figure 1: Feynman diagrams corresponding to the generation of the masses of the charged fermions as well as for the Dirac neutrino submatrix. The charged fermions of the first and second generations get their masses via seesaw-like diagrams mediated by ψ_1 and ψ_2, whereas those of the third generation get their masses through their Yukawa couplings to Φ and Σ fields.

The 3×3 sub-matrices $M_c^{(u,d,e,\nu)}$ in Eqs. 6 and 7 have only the $(3,3)$ element as non-zero and are given as

$$\left(M_c^{(u)}\right)_{ij} = \frac{1}{\sqrt{2}}\left(y_3 v_1 + x_3 v_{\Sigma_1}\right)\delta_{i3}\delta_{j3}, \qquad \left(M_c^{(d)}\right)_{ij} = \frac{1}{\sqrt{2}}\left(y_3 v_2 + x_3 v_{\Sigma_2}\right)\delta_{i3}\delta_{j3}, \tag{9}$$

$$\left(M_c^{(e)}\right)_{ij} = \frac{1}{\sqrt{2}}\left(y_3 v_2 - 3x_3 v_{\Sigma_2}\right)\delta_{i3}\delta_{j3}, \qquad (M_c^{(\nu)})_{ij} = \frac{1}{\sqrt{2}}\left(y_3 v_1 - 3x_3 v_{\Sigma_1}\right)\delta_{i3}\delta_{j3}, \tag{10}$$

and these correspond to the masses of the third families of fermions generated from their Yukawa couplings to Φ and Σ. The remaining sub-matrices appearing in the quark sector are given as,

$$M_a^{(u)} = \frac{1}{\sqrt{2}}\begin{pmatrix} \left(y_1 v_1 + x_1 v_{\Sigma_1}\right) Y_{\mathbf{2},2}^{(2)}(\tau) & \left(y_2 v_1 + x_2 v_{\Sigma_1}\right) Y_{\mathbf{2},2}^{(4)}(\tau) \\ -\left(y_1 v_1 + x_1 v_{\Sigma_1}\right) Y_{\mathbf{2},1}^{(2)}(\tau) & -\left(y_2 v_1 + x_2 v_{\Sigma_1}\right) Y_{\mathbf{2},1}^{(4)}(\tau) \\ 0 & 0 \end{pmatrix}, \tag{11}$$

$$M_b^{(u)} = \frac{1}{\sqrt{2}}\begin{pmatrix} Y_{\mathbf{1}'}^{(6)}\left(z_1 v_{\sigma_1} + w_1 v_{\Xi_1}\right) & Y_{\mathbf{1}}^{(4)}(\tau)\left(z_2 v_{\sigma_1} + w_2 v_{\Xi_1}\right) & Y_{\mathbf{1}}^{(4)}(\tau)\left(z_3 v_{\sigma_2} + w_3 v_{\Xi_2}\right) \\ 0 & z_4 v_{\sigma_2} + w_4 v_{\Xi_2} & Y_{\mathbf{1}}^{(4)}(\tau)\left(z_5 v_{\sigma_1} + w_5 v_{\Xi_1}\right) \end{pmatrix} = M_b^{(d)}, \tag{12}$$

$$M_a^{(d)} = \frac{1}{\sqrt{2}}\begin{pmatrix} \left(y_1 v_2 + x_1 v_{\Sigma_2}\right) Y_{\mathbf{2},2}^{(2)}(\tau) & \left(y_2 v_2 + x_2 v_{\Sigma_2}\right) Y_{\mathbf{2},2}^{(4)}(\tau) \\ -\left(y_1 v_2 + x_1 v_{\Sigma_2}\right) Y_{\mathbf{2},1}^{(2)}(\tau) & -\left(y_2 v_2 + x_2 v_{\Sigma_2}\right) Y_{\mathbf{2},1}^{(4)}(\tau) \\ 0 & 0 \end{pmatrix}, \tag{13}$$

whereas those in the lepton sector are given as,

$$M_a^{(e)} = \frac{1}{\sqrt{2}}\begin{pmatrix} \left(y_1 v_2 - 3x_1 v_{\Sigma_2}\right) Y_{\mathbf{2},2}^{(2)}(\tau) & \left(y_2 v_2 - 3x_2 v_{\Sigma_2}\right) Y_{\mathbf{2},2}^{(4)}(\tau) \\ -\left(y_1 v_2 - 3x_1 v_{\Sigma_2}\right) Y_{\mathbf{2},1}^{(2)}(\tau) & -\left(y_2 v_2 - 3x_2 v_{\Sigma_2}\right) Y_{\mathbf{2},1}^{(4)}(\tau) \\ 0 & 0 \end{pmatrix}, \tag{14}$$

$$M_b^{(e)} = \frac{1}{\sqrt{2}} \begin{pmatrix} Y_{\mathbf{1}'}^{(6)} \left(z_1 v_{\sigma_1} - 3w_1 v_{\Xi_1}\right) & Y_{\mathbf{1}}^{(4)}(\tau)\left(z_2 v_{\sigma_1} - 3w_2 v_{\Xi_1}\right) & Y_{\mathbf{1}}^{(4)}(\tau)\left(z_3 v_{\sigma_2} - 3w_3 v_{\Xi_2}\right) \\ 0 & z_4 v_{\sigma_2} - 3w_4 v_{\Xi_2} & Y_{\mathbf{1}}^{(4)}(\tau)\left(z_5 v_{\sigma_1} - 3w_5 v_{\Xi_1}\right) \end{pmatrix} = M_b^{(\nu)}, \tag{15}$$

$$M_a^{(\nu)} = \frac{1}{\sqrt{2}} \begin{pmatrix} \left(y_1 v_1 - 3x_1 v_{\Sigma_1}\right) Y_{\mathbf{2},2}^{(2)}(\tau) & \left(y_2 v_1 - 3x_2 v_{\Sigma_1}\right) Y_{\mathbf{2},2}^{(4)}(\tau) \\ -\left(y_1 v_1 - 3x_1 v_{\Sigma_1}\right) Y_{\mathbf{2},1}^{(2)}(\tau) & -\left(y_2 v_1 - 3x_2 v_{\Sigma_1}\right) Y_{\mathbf{2},1}^{(4)}(\tau) \\ 0 & 0 \end{pmatrix}. \tag{16}$$

Thus, once we integrate out the heavy vector like fermions Ψ_1 and Ψ_2, the masses for the first and second generation of the SM charged fermions are obtained via Seesaw mechanism, which also yields the Dirac neutrino sub-matrix, $\widetilde{M}_\nu$. The resulting effective low energy 3×3 mass matrices for the SM charged fermions as well as the Dirac neutrino matrix are:

$$\widetilde{M}_u = M_c^{(u)} - M_a^{(u)} M_U^{-1} M_b^{(u)}\,, \qquad \widetilde{M}_d = M_c^{(d)} - M_a^{(d)} M_D^{-1} M_b^{(d)}\,, \tag{17}$$

$$\widetilde{M}_e = M_c^{(e)} - M_a^{(e)} M_E^{-1} M_b^{(e)}\,, \qquad \widetilde{M}_\nu = M_c^{(\nu)} - M_a^{(\nu)} M_N^{-1} M_b^{(\nu)}\,. \tag{18}$$

As mentioned before, our model also contains extra singlet fermions S_i^c that couple to the right handed neutrinos ν^c (last two lines in Eq.5). Thus the resultant neutral fermion mass terms (after integrating out the Ψ fields) can be written as,

$$\frac{1}{2}\begin{pmatrix} \nu & \nu^c & S^c \end{pmatrix} \begin{pmatrix} 0_{3\times3} & \widetilde{M}_\nu & 0_{3\times3} \\ \widetilde{M}_\nu^T & 0_{3\times3} & M_R \\ 0_{3\times3} & M_R^T & M_S \end{pmatrix} \begin{pmatrix} \nu \\ \nu^c \\ S^c \end{pmatrix} + \text{h.c.}. \tag{19}$$

In the above equation, all the sub-matrices are 3×3 with the Dirac mass matrix $\widetilde{M}_\nu$ determined by Eq. 18, while M_R and M_S are given as

$$M_R = \begin{pmatrix} \gamma_1 Y_{\mathbf{2},1}^{(4)}(\tau) & \gamma_1 Y_{\mathbf{2},2}^{(4)}(\tau) & 0 \\ -\gamma_2 Y_{\mathbf{2},2}^{(2)}(\tau) & \gamma_2 Y_{\mathbf{2},1}^{(2)}(\tau) & 0 \\ -\gamma_3 Y_{\mathbf{2},2}^{(4)}(\tau) & \gamma_3 Y_{\mathbf{2},1}^{(4)}(\tau) & \gamma_4 Y_{\mathbf{1}}^{(4)}(\tau) \end{pmatrix} \frac{v_R}{\sqrt{2}}, \quad M_S = \begin{pmatrix} -M_1 Y_{\mathbf{2},1}^{(2)}(\tau) & M_1 Y_{\mathbf{2},2}^{(2)}(\tau) & -M_2 Y_{\mathbf{2},2}^{(2)}(\tau) \\ M_1 Y_{\mathbf{2},2}^{(2)}(\tau) & M_1 Y_{\mathbf{2},1}^{(2)}(\tau) & M_2 Y_{\mathbf{2},1}^{(2)}(\tau) \\ -M_2 Y_{\mathbf{2},2}^{(2)}(\tau) & M_2 Y_{\mathbf{2},1}^{(2)}(\tau) & 0 \end{pmatrix}. \tag{20}$$

In the limit $M_S \gg M_R \gg \widetilde{M}_\nu$, the mass matrix in Eq.19 corresponds to the double seesaw[33], [1] according to which, once the heavy fields ν^c and S^c are integrated out, the mass matrix for the light active neutrinos reads:

$$M_\nu = \widetilde{M}_\nu M_R^{-1} M_S M_R^{-1} \widetilde{M}_\nu^T\,. \tag{21}$$

III. NUMERICAL ANALYSIS

In this section, we present the results of the numerical analysis conducted to evaluate the viability of the model in explaining the observed fermion masses and mixing. We vary all input parameters, including Yukawa couplings, *vevs* and masses, and minimize the function χ^2, which is defined as

$$\chi^2 = \sum_i \left(\frac{O_{i_{\rm calc}} - O_{i_{\rm exp}}}{O_{i_{\rm exp}}}\right)^2, \tag{22}$$

to determine the best fit parameters that reproduce the observed fermion masses and mixing.

[1] For a seesaw review see e.g. [34].

Input Parameters	Best fit value for NH of light neutrinos
τ	$-0.03224\ +\ i\ 1.86682$
m_{Ψ_1}, m_{Ψ_2} (GeV)	2.38×10^{12}, 8.71×10^{12}
v_1, v_2 (GeV)	245.62150, 3.95665
$v_{\Sigma_1}, v_{\Sigma_2}$ (GeV)	8.37732, 10.01214
$v_{\sigma_1}, v_{\sigma_2}$ (GeV)	6.12×10^{12}, 4.64×10^{12}
v_{Ξ_1}, v_{Ξ_2} (GeV)	7.90×10^{12}, 3.53×10^{12}
v_R (GeV)	1.23×10^{11}
M_1, M_2 (GeV)	1.0×10^{12}, 6.20×10^{8}
x_1, x_2, x_3	$3.53382\ e^{i\ 2.23402}$, $2.93598\ e^{i\ 3.85910}$, $0.20033\ e^{i\ 2.15046}$
y_1, y_2, y_3	$0.27120\ e^{i\ 5.93154}$, $0.46397\ e^{i\ 5.47007}$, $0.98750\ e^{i\ 2.24996}$
w_1, w_2, w_3, w_4, w_5	$0.75168\ e^{i\ 0.96442}$, $0.20136\ e^{i\ 2.04578}$, $1.37663\ e^{i\ 5.91647}$, $0.23368\ e^{i\ 0.86247}$, $2.62639\ e^{i\ 5.87924}$
z_1, z_2, z_3, z_4, z_5	$2.37549\ e^{i\ 0.67600}$, $0.25164\ e^{i\ 1.45687}$, $2.46850\ e^{i\ 4.02943}$, $0.32353\ e^{i\ 0.15040}$, $3.54392\ e^{i\ 6.12983}$
$\gamma_1, \gamma_2, \gamma_3, \gamma_4$	$0.20302\ e^{i\ 3.09154}$, $1.99746\ e^{i\ 6.05522}$, $3.42165\ e^{i\ 0.22612}$, $1.96501\ e^{i\ 5.93289}$
$M_{\text{heavy neutrinos}}$ (GeV)	6.06521×10^{5}, 2.49460×10^{9}, 2.64148×10^{9}, 3.95307×10^{9}, 1.25075×10^{11}, 1.28998×10^{11}
	Low energy mass matrices, masses and mixing parameters
$\widetilde{M}_u$ (GeV)	$\begin{pmatrix} -0.00018e^{i(-2.57621)} & -0.01312e^{i2.50106} & 0.00174e^{i1.43459} \\ 0.00428e^{i0.66665} & -0.19406e^{i2.37489} & -0.06547e^{i(-2.04282)} \\ 0.00000e^{i0.00000} & 0.00000e^{i0.00000} & -108.38236e^{i2.24928} \end{pmatrix}$
$\widetilde{M}_d$ (GeV)	$\begin{pmatrix} 0.00016e^{i(-0.36728)} & 0.00339e^{i0.98476} & -0.00459e^{i(-2.87477)} \\ -0.00409e^{i2.87558} & -0.00659e^{i1.86300} & 0.15841e^{i0.40887} \\ 0.00000e^{i0.00000} & 0.00000e^{i0.00000} & -2.51228e^{i2.21622} \end{pmatrix}$
m_u, m_c, m_t (GeV)	0.00054, 0.2670, 172.69001
m_d, m_s, m_b (GeV)	0.00120, 0.0240, 4.180
$s^q_{12}, s^q_{23}, s^q_{13}, \delta^q_{CP}$	0.2250, 0.04182, 0.00370, 65.6750°
$\widetilde{M}_e$ (GeV)	$\begin{pmatrix} 0.00011e^{i0.67714} & -0.00335e^{i1.79184} & 0.02874e^{i(-0.74991)} \\ -0.00261e^{i(-2.36319)} & -0.10577e^{i(-2.70883)} & -0.64387e^{i2.36816} \\ 0.00000e^{i0.00000} & 0.00000e^{i0.00000} & 0.59512e^{i(-1.17142)} \end{pmatrix}$
M_ν (eV)	$\begin{pmatrix} 0.00013e^{i0.26925} & 0.00065e^{i(-1.25936)} & 0.00314e^{i0.96134} \\ 0.00065e^{i(-1.25936)} & -0.02407e^{i2.14357} & 0.01431e^{i(-0.64736)} \\ 0.00314e^{i0.96134} & 0.01431e^{i(-0.64736)} & 0.00000e^{i0.00000} \end{pmatrix}$
m_e, m_μ, m_τ (GeV)	0.00048, 0.10155, 1.77686
m_{ν_1}(eV), Δm^2_{sol}, Δm^2_{atm}(eV^2)	0.00276, 7.49×10^{-5}, 0.00251
$s^\nu_{12}, s^\nu_{23}, s^\nu_{13}$	0.55497, 0.68557, 0.14883
$\delta^\nu_{CP}, \alpha^M, \beta^M$	323.53560°, 194.46228°, 297.46063°

Table II: Sample best fit input parameters for NH of active neutrinos along with the corresponding values of the calculated fermion masses and mixing parameters. The χ^2 value for the given point is 6.30442×10^{-15}. The low-energy mass matrices for the up and down type quarks, charged leptons, and active light neutrinos as well as the masses of the heavy neutrinos in addition to the ones coming from $\Psi_{1,2}$ are also given. For the PMNS matrix, the Majorana phase matrix is defined as $P=\text{diagonal}\ (1, e^{i\alpha^M/2}, e^{i\beta^M/2})$.

In Eq.22, $O_{i_{\text{calc}}}$ represents the model prediction, while $O_{i_{\text{exp}}}$ denotes the experimental best fit value. The summation is performed over the masses of charged fermions [35, 36], the CKM mixing angles, the CKM CP phase, the PMNS mixing angles, and the mass-squared differences of light neutrinos [37, 38]. While fitting the charged fermion masses, the masses of the first two generations are fitted at 10^{12}GeV [35], as they arise from the seesaw mechanism, while those of the third generation are taken at the electroweak scale [36]. In addition, the constraint from cosmological observations on the sum of the active light neutrino masses, $\Sigma m_i \leq 0.12$ eV [39], as well as the 3σ bound on the CP phase of the PMNS matrix [37, 38], are imposed as extra conditions. In our fit, the absolute values of the Yukawa couplings are taken to be within the range $[0.2, \sqrt{4\pi}]$, whereas their phases are varied in the range $[0, 2\pi]$. An important result is that the model only fits the Normal Ordering (NO) of the active light neutrino masses, whereas the Inverted Ordering (IO) is disfavored.

In Table II, we present a set of sample best fit parameters that reproduce the correct fermion masses and mixing along with the corresponding values of the calculated fermion masses and mixing parameters. The low-energy mass matrices for the up- and down-type quarks, charged leptons, and active light neutrinos are also given in this table. One can see that the rows of the charged fermion mass matrices satisfy a natural hierarchy as a consequence of the modular symmetry with two family seesaw, which in turn explains the observed fermion mass hierarchy.

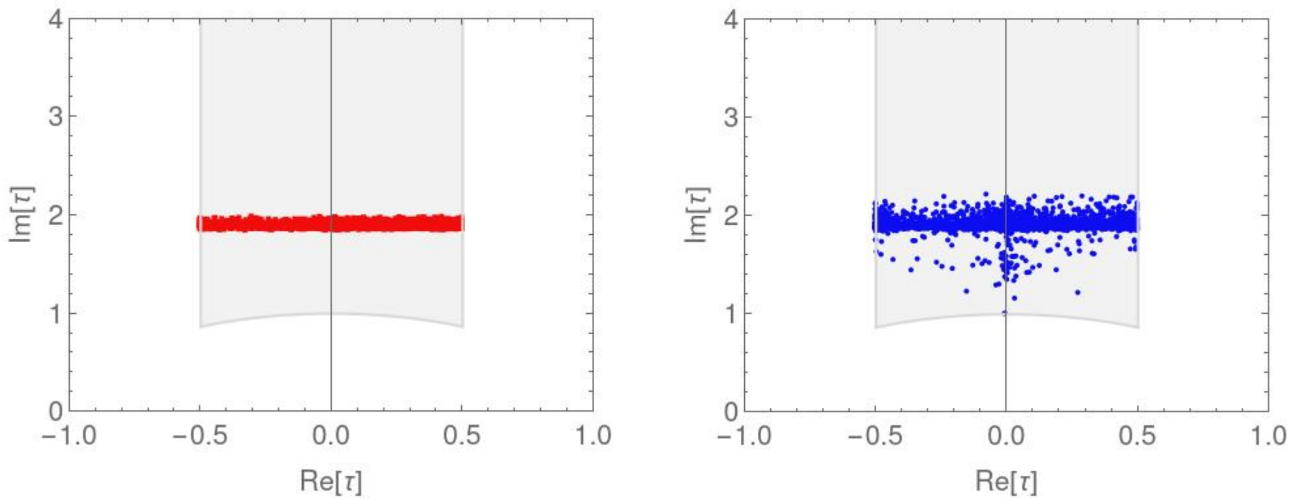

Figure 2: The values of the real and imaginary components of the modular field τ that give $\chi^2 <= 5\times 10^{-4}$ in our numerical scan. The fundamental domain for τ $\left(-\frac{1}{2} \leq \mathrm{Re}[\tau] \leq \frac{1}{2}, \quad |\tau| \leq 1\right)$ is shown by the gray-shaded region. The left panel is for fixed *vevs* and mass scales whereas they are varied in the right panel. See text for details.

In Fig.2, we show the values of the real and imaginary components of the modular field τ that give $\chi^2 <= 5\times 10^{-4}$ in our numerical scan. In the left panel, the masses of the seesaw mediators and the *vevs* are fixed according to the values provided in Table II, while the absolute values of the Yukawa couplings are varied within the range $[0.2, \sqrt{4\pi}]$, with their phases taking any value within $[0, 2\pi]$. In the right panel, both the mediator masses and the *vevs* are also varied freely in addition to the Yukawa couplings. The fundamental domain of τ, $\left(-\frac{1}{2} \leq \mathrm{Re}[\tau] \leq \frac{1}{2}, \quad |\tau| \geq 1\right)$ is shown by the gray-shaded region. From the figure, one can see that the imaginary part of τ (τ_I) is more restricted than the real part (τ_R). This is because the magnitudes of the entries of the fermion mass matrices are more sensitive to τ_I than to τ_R. This can be seen for instance, by taking the $(1,1)$ entry of $\widetilde{M}_u$ to the leading order in the q - expansion of the modular forms,

$$(\widetilde{M}_u)_{11} \approx -\frac{9e^{-6\pi\tau_I+2i\pi\tau_R}\left(e^{4\pi\tau_I}-16e^{2\pi(\tau_I+i\tau_R)}+576e^{4i\pi\tau_R}\right)(v_{\Sigma 1}x_1+v_1y_1)(v_{\Xi 1}w_1+v_{\Sigma 1}z_1)}{128M_1}, \tag{23}$$

from which we can see that τ_R always contribute to the phases of the individual terms in the expansion. The same goes for all the mass terms. This is the reason why τ_I is restricted to be in the range $\sim [1.8, 2]$ for the case of fixed mass scales and *vevs* (left panel of Fig.2) as the fermion masses and mixing are more sensitive to τ_I. The variation in the mass scales and the *vevs* can relax this bound because the variation in the absolute values of the mass terms due to τ_I can be compensated by taking different *vevs* and/or mass scales.

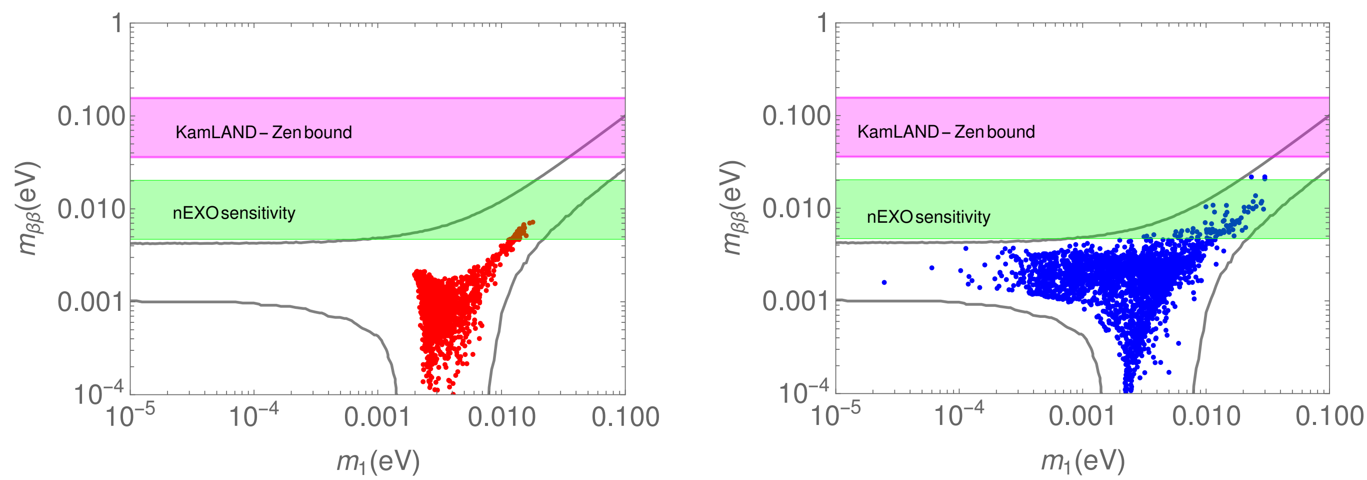

Figure 3: Predictions for the effective Majorana mass (m_{ee}) governing $0\nu\beta\beta$. The region within the solid gray lines represents the standard predictions for m_{ee} assuming the active light neutrinos follow the normal hierarchy. The left and right panels correspond to the cases with fixed and varying mass scales, respectively, as in Fig. 2. The region above the purple band is excluded by the KamlAND-Zen experimental bound, while the green band corresponds to the projected sensitivity of the nEXO experiment.

Fig.3 shows the predictions for the effective Majorana mass (m_{ee}) that governs $0\nu\beta\beta$. Note that we have shown only the contributions due to the three active light neutrinos since the mixing of the heavy neutrinos with the active light neutrinos is strongly suppressed, making their contribution to $0\nu\beta\beta$ negligible. The region within the solid gray lines represents the standard predictions for m_{ee}, with the assumption that the active light neutrinos follow the normal hierarchy and no modular symmetry. The red/blue points indicate the predictions from our model. As in Fig.2, the masses of the seesaw mediators and the *vev*s are fixed according to the values provided in Table II in the left panel, while the magnitude and phase of the Yukawa couplings are varied within the ranges $[0.2, \sqrt{4\pi}]$ and $[0, 2\pi]$, respectively. In the right panel, both the mediator masses and the *vev*s are allowed to vary freely in addition to the Yukawa couplings. The region above the purple band is excluded by the experimental bound from KamlAND-Zen [40], while the green band corresponds to the projected sensitivity of the nEXO experiment [41]. The widths of these bands are due to the uncertainty in the values of the nuclear matrix elements. One interesting feature that we can see from this figure is that the model predicts a lower bound on the mass of the lightest active neutrino. This is around 0.0025 eV for the case of fixed mass scales while it becomes $\sim 10^{-4}$ eV in the general case. A small part of the predicted parameter space lies within the nEXO reach.

Fig.4 shows the correlations of the Dirac CP phase δ^{ν}_{CP} and one of the Majorana phases, α, to the lightest neutrino mass m_1. As before, the left and right panels correspond to the cases with fixed and varying mass scales, respectively. It is interesting to see that for the case of fixed scales, there exists a strong correlation between m_1 and δ^{ν}_{CP} as well as α, in particular for the case of fixed mass scales. Moreover, the Dirac CP violating neutrino oscillation phase is found to lie in the range $\delta^{\nu}_{\rm CP} \sim 260^o - 360^o$.

IV. CONCLUSIONS

We have proposed a model based on the smallest quark-lepton unified symmetry, the Pati-Salam gauge group and the smallest modular symmetry, S_3. The masses of the third family of SM charged fermion arise from renormalisable Yukawa interactions involving a colourless scalar bi-doublet as well as a bi-doublet scalar in the adjoint representation of $SU(4)_C$. The first and second family masses are naturally suppressed due to a Pati-Salam version of the type

I seesaw mechanism for neutrinos, but here mediated through heavier vector-like Pati-Salam fermions. Due to the Pati-Salam symmetry, the same mechanism also suppresses first and second family Dirac neutrino masses, but in the neutrino sector there are additional fields leading to tiny active Majorana neutrino masses via a Double Seesaw mechanism.

The diagrams responsible for the effective Yukawa operators are similar to those of the type I seesaw mechanism for neutrinos, with two insertions of vacuum expectation values, where one of them breaks electroweak symmetry, and one does not. The three Pati-Salam families are essentially distinguished by whether they couple to heavier vector-like fermions (the first two families) or not (third family), and this is controlled by their S_3 assignments. The modular S_3 is perfect for implementing such a two-family seesaw mechanism, since it admits doublet representations for the first two families, and a singlet representation for the third family.

The model is shown to describe all quark and lepton (including neutrino) masses and mixing angles, in terms of high energy mass scales, together with complex dimensionless Yukawa coefficients which are all of order unity, and a single complex modulus field τ with $\mathrm{Im}(\tau) \sim 2$. It provides a good fit to neutrino data, assuming a normal ordering of neutrino masses, while the inverted ordering is disfavoured. The associated prediction for neutrinoless double beta decay is partly within the reach of the nEXO experiment. In particular, the Dirac CP violating neutrino oscillation phase is predicted to lie in the range $\delta^{\nu}_{\mathrm{CP}} \sim 260^o - 360^o$.

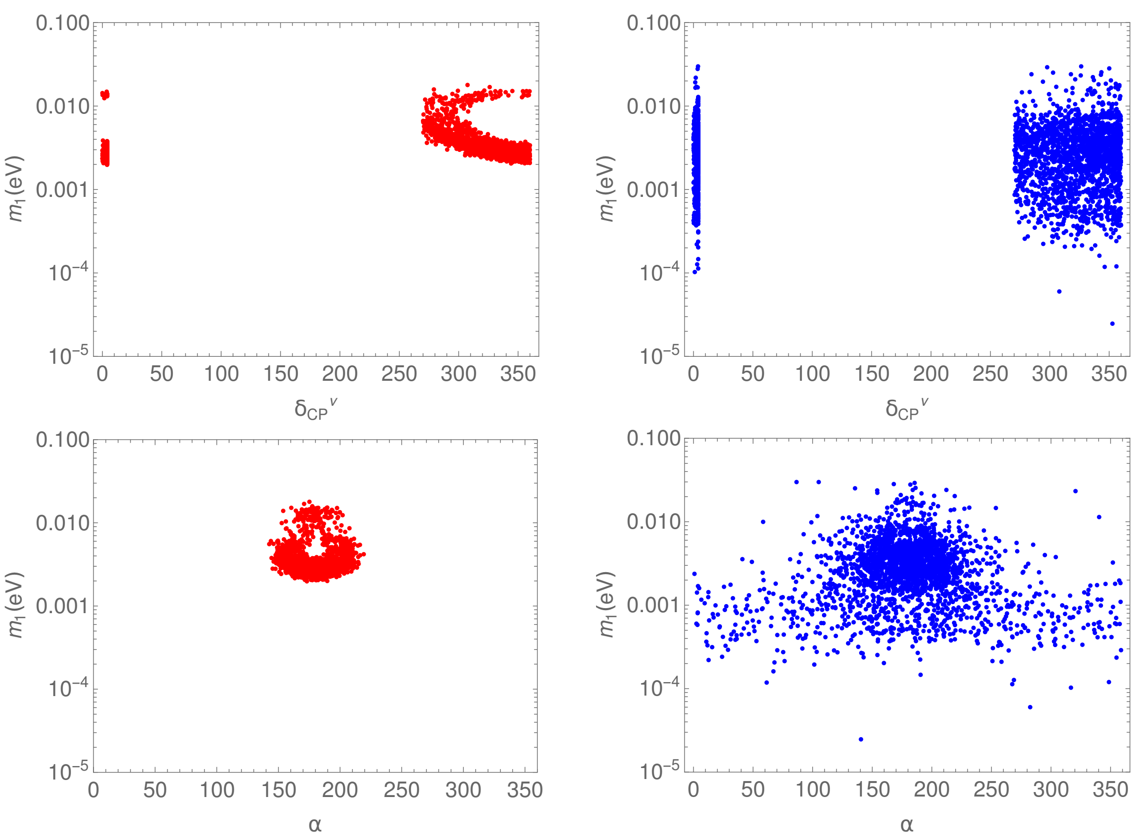

Figure 4: Correlations of the Dirac CP phase δ^{ν}_{CP} and the Majorana phase α to the lightest neutrino mass m_1. The left and right panels correspond to the cases with fixed and varying mass scales, respectively, as in the previous figures.

Acknowledgments

A.E.C.H is supported by ANID-Chile FONDECYT 1210378, ANID-Chile FONDECYT 1241855, ANID PIA/APOYO AFB230003 and ANID- Programa Milenio - code ICN2019_044. V.K.N. is supported by ANID-Chile Fondecyt Post-doctoral grant 3220005. IdMV acknowledges funding from Fundação para a Ciência e a Tecnologia (FCT) through the projects CFTP-FCT Unit UIDB/FIS/00777/2020 and UIDP/FIS/00777/2020, CERN/FIS-PAR/0019/2021, CERN/FIS-PAR/0002/2021, 2024.02004 CERN, which are partially funded through POCTI (FEDER), COMPETE, QREN and EU. A.E.C.H. thanks the Instituto Superior Técnico, Universidade de Lisboa for hospitality, where part of this work was done. S.F.K. acknowledges the STFC Consolidated Grant ST/X000583/1 and the European Union's Horizon 2020 Research and Innovation programme under the Marie Sklodowska-Curie grant agreement HIDDeN European ITN project (H2020-MSCA-ITN-2019//860881-HIDDeN).

Appendix A: Modular flavor symmetry

In this appendix, we provide a concise review of the main features of modular flavor symmetry. The full modular group $\Gamma \cong \mathrm{SL}(2,\mathbb{Z})$ corresponds to the group of two-dimensional matrices with integral entries and unit determinant,

$$\Gamma = \left\{ \begin{pmatrix} a & b \\ c & d \end{pmatrix} \Big| a, b, c, d \in \mathbb{Z}, \quad ad - bc = 1 \right\} . \tag{A1}$$

The modular group is an infinite group that can be generated by two elements, conventionally denoted as:

$$S = \begin{pmatrix} 0 & 1 \\ -1 & 0 \end{pmatrix}, \quad T = \begin{pmatrix} 1 & 1 \\ 0 & 1 \end{pmatrix}, \tag{A2}$$

which fulfill the relations:

$$S^4 = (ST)^3 = 1, \quad S^2 T = T S^2 . \tag{A3}$$

The modular symmetry is ubiquitous in string compactifications and corresponds to the geometrical symmetry of the extra compact space. In simple toroidal compactification, the two-dimensional torus T^2 is described as the quotient $T^2 = \mathbb{C}/\Lambda_{\omega_1,\omega_2}$, where $\mathbb{C}$ stands for the whole complex plane $\mathbb{C}$ and $\Lambda_{\omega_1,\omega_2} = \{m\omega_1 + n\omega_2, m, n \in \mathbb{Z}\}$ denotes a two-dimensional lattice with the basis vectors ω_1 and ω_2. The lattice is left invariant under a change in lattice basis vectors only and if only

$$\begin{pmatrix} \omega_1 \\ \omega_2 \end{pmatrix} \to \begin{pmatrix} \omega_1' \\ \omega_2' \end{pmatrix} = \begin{pmatrix} a & b \\ c & d \end{pmatrix} \begin{pmatrix} \omega_1 \\ \omega_2 \end{pmatrix}, \qquad \begin{pmatrix} a & b \\ c & d \end{pmatrix} \in \Gamma . \tag{A4}$$

The torus is characterized by the complex modulus $\tau = \omega_1/\omega_2$ up to rotation and scale transformations, without loss of generality we can limit τ to the upper half of the complex plane with $\mathrm{Im}(\tau) > 0$. The two tori related by modular transformations would be identical, i.e.

$$\tau \xrightarrow{\gamma} \tau' = \frac{\omega_1'}{\omega_2'} = \frac{a\tau + b}{c\tau + d} \equiv \gamma\tau, \quad \mathrm{Im}(\tau) > 0, \quad \gamma = \begin{pmatrix} a & b \\ c & d \end{pmatrix} . \tag{A5}$$

Thus the action of the generators S and T, corresponding to modular inversion and translation respectively, take the form:

$$\tau \xrightarrow{S} -\frac{1}{\tau}, \quad \tau \xrightarrow{T} \tau + 1 . \tag{A6}$$

Notice that $\gamma \in \Gamma$ and $-\gamma \in \Gamma$ define the same transformation of τ. Making use of the modular transformations, it is always possible to restrict τ to the fundamental domain defined as follows:

$$\mathcal{D} = \left\{ \tau \,\middle|\, \mathrm{Im}(\tau) > 0, |\mathrm{Re}(\tau)| \leq \frac{1}{2}, |\tau| \geq 1 \right\} .$$

Any value of τ in the upper-half plane can be mapped into the fundamental domain $\mathcal{D}$ by performing an appropriate modular transformation, but no two points inside the fundamental domain $\mathcal{D}$ are related under the modular group. Consequently, the fundamental domain $\mathcal{D}$ is a representative set of the physically inequivalent modulus. Notice that the left boundary of $\mathcal{D}$ with $\mathrm{Re}(\tau) = -1/2$ is related to the right boundary of $\mathrm{Re}(\tau) = 1/2$ by the T transformation, and the S transformation maps the left unit arc $\tau = e^{i\theta}(\pi/2 \leq \theta \leq 2\pi/3)$ on the boundary is related to the right unit arc $\tau = e^{i\theta}(\pi/3 \leq \theta \leq \pi/2)$ by the S transformation.

The modular symmetry provides an origin of the discrete flavor symmetry through the quotient,

$$\Gamma_N = \Gamma / \pm \Gamma(N), \quad \Gamma'_N = \Gamma/\Gamma(N) \,, \tag{A7}$$

where Γ_N and Γ'_N are the inhomogeneous and homogeneous finite modular groups respectively, and $\Gamma(N)$ is the principal normal subgroup of level N,

$$\Gamma(N) = \left\{ \begin{pmatrix} a & b \\ c & d \end{pmatrix} \in \Gamma, \begin{pmatrix} a & b \\ c & d \end{pmatrix} = \begin{pmatrix} 1 & 0 \\ 0 & 1 \end{pmatrix} \pmod{N} \right\} , \tag{A8}$$

which implies $T^N \in \Gamma(N)$. The inhomogeneous finite modular groups Γ_N for $N = 2, 3, 4, 5$ are isomorphic to the permutation groups S_3, A_4, S_4 and A_5 respectively [1, 42], and Γ'_N is the double cover of Γ_N [6].

In the framework of $\mathcal{N} = 1$ global supersymmetry, the modulus τ is a chiral supermultiplet and its scalar component is restricted to the upper half of the complex plane, and the action takes the form

$$\mathcal{S} = \int d^4x d^2\theta d^2\bar{\theta}\, \mathcal{K}(\tau, \bar{\tau}; \Phi_I, \bar{\Phi}_I) + \left[\int d^4x d^2\theta\, \mathcal{W}(\tau, \Phi_I) + \text{h.c.} \right] , \tag{A9}$$

where the Kähler potential $\mathcal{K}(\tau, \bar{\tau}; \Phi_I, \bar{\Phi}_I)$ is a real gauge-invariant function of the chiral superfields τ, Φ_I and their conjugates, the superpotential $\mathcal{W}(\tau, \Phi_I)$ is a holomorphic gauge invariant function of the chiral superfields τ, Φ_I. Under the action of $\gamma \in \Gamma$, the superfield Φ_I have the following non-linear transformation:

$$\Phi_I \xrightarrow{\gamma} (c\tau + d)^{-k_I} \rho_I(\gamma) \Phi_I \,, \tag{A10}$$

where the weight k_I is an integer and ρ_I is a unitary representation of the finite modular group Γ_N or Γ'_N. The Kähler potential is assumed to take the following minimal form

$$\mathcal{K}(\tau, \bar{\tau}; \Phi_I, \bar{\Phi}_I) = -h \log(-i\tau + i\bar{\tau}) + \sum_I \frac{\bar{\Phi}_I \Phi_I}{(-i\tau + i\bar{\tau})^{k_I}} \,, \tag{A11}$$

which is invariant up to Kähler transformations. It yields the kinetic terms of for the scalar components of τ and Φ_I after the modulus acquire a *vev*.

In the concerning to the superpotential $\mathcal{W}(\tau, \Phi_I)$, it can be expressed as follows

$$\mathcal{W}(\tau, \Phi_I) = \sum_n Y_{I_1 \ldots I_n}(\tau) \Phi_{I_1} \ldots \Phi_{I_n} \,. \tag{A12}$$

Modular invariance of $\mathcal{W}$ requires that $Y_{I_1 \ldots I_n}(\tau)$ should be a modular form of weight k_Y and level N transforming in the representation ρ_Y of Γ_N (or Γ'_N), i.e.,

$$Y_{I_1 \ldots I_n}(\tau) \xrightarrow{\gamma} Y_{I_1 \ldots I_n}(\gamma\tau) = (c\tau + d)^{k_Y} \rho_Y(\gamma) Y_{I_1 \ldots I_n}(\tau) \,. \tag{A13}$$

The modular weights and the representations should fullfill the following conditions

$$k_Y = k_{I_1} + \ldots + k_{I_n}\,, \qquad \rho_Y \otimes \rho_{I_1} \otimes \ldots \otimes \rho_{I_n} \supset \mathbf{1}\,, \tag{A14}$$

where $\mathbf{1}$ denotes the trivial singlet of Γ_N (or Γ'_N).

In the present work, we shall concerned with the inhomogeneous finite modular group S_3. The group $\Gamma_2 \cong S_3$ is the permutation group of order 3 with 6 elements, which can be expressed in terms of the two S and T generators satisfying the following relations [43]:

$$S^2 = T^2 = (ST)^3 = 1\,. \tag{A15}$$

The six elements of $\Gamma_2 \cong S_3$ can be grouped into three conjugacy classes

$$1C_1 = \{1\}\,, \quad 3C_2 = \{S, T, TST\}, \quad 2C_3 = \{ST, TS\}\,, \tag{A16}$$

where nC_k stands for the conjugacy class of k elements of order n. The irreducible representations of the finite modular S_3 group are two singlets $\mathbf{1}$ and $\mathbf{1'}$, and one doublet $\mathbf{2}$. Here we work in the basis of diagonal matrix representation for the T generator. The representation matrices for the S and T generators in the three S_3 irreducible representations take the form:

$$\begin{aligned}
\mathbf{1} &: \quad \rho_{\mathbf{1}}(S) = 1, \qquad \rho_{\mathbf{1}}(T) = 1\,, \\
\mathbf{1'} &: \quad \rho_{\mathbf{1'}}(S) = -1, \qquad \rho_{\mathbf{1'}}(T) = -1\,, \\
\mathbf{2} &: \quad \rho_{\mathbf{2}}(S) = -\frac{1}{2}\begin{pmatrix} 1 & \sqrt{3} \\ \sqrt{3} & -1 \end{pmatrix}, \qquad \rho_{\mathbf{2}}(T) = \begin{pmatrix} 1 & 0 \\ 0 & -1 \end{pmatrix}.
\end{aligned} \tag{A17}$$

The tensor product rules between the S_3 irreducible representations are given by:

$$\mathbf{1} \otimes \mathbf{1'} = \mathbf{1'}, \qquad \mathbf{1^a} \otimes \mathbf{2} = \mathbf{2}, \qquad \mathbf{2} \otimes \mathbf{2} = \mathbf{1} \oplus \mathbf{1'} \oplus \mathbf{2}\,, \tag{A18}$$

where $a, b = 0, 1$ and we denote $\mathbf{1^0} \equiv \mathbf{1}$ and $\mathbf{1^1} \equiv \mathbf{1'}$. Regarding the product of the singlet $\mathbf{1'}$ with a doublet, we have

$$\mathbf{1'} \otimes \mathbf{2} = \mathbf{2} \;\sim \theta \begin{pmatrix} \varphi_2 \\ -\varphi_1 \end{pmatrix}. \tag{A19}$$

Whereas the tensor product rule of two S_3 doublets takes the form:

$$\mathbf{2} \otimes \mathbf{2} = \mathbf{1} \oplus \mathbf{1'} \oplus \mathbf{2}, \qquad \text{with} \qquad \begin{cases} \mathbf{1} \;= \theta_1\varphi_1 + \theta_2\varphi_2\,, \\ \mathbf{1'} = \theta_1\varphi_2 - \theta_2\varphi_1\,, \\ \mathbf{2} \;= \begin{pmatrix} \theta_2\varphi_2 - \theta_1\varphi_1 \\ \theta_1\varphi_2 + \theta_2\varphi_1 \end{pmatrix}. \end{cases}$$

In the finite modular S_3 group, there are two linearly independent modular forms of the lowest non-trivial weight 2, which can be accommodated into a S_3 doublet $\mathbf{2}$ of S_3 and the doublet is given by:

$$Y_{\mathbf{2}}^{(2)} = \begin{pmatrix} Y_1(\tau) \\ Y_2(\tau) \end{pmatrix}. \tag{A20}$$

where the modular forms $Y_1(\tau)$ and $Y_2(\tau)$ take the form [44]:

$$\begin{aligned}
Y_1(\tau) &= \frac{i}{4\pi}\left[\frac{\eta'(\tau/2)}{\eta(\tau/2)} + \frac{\eta'((\tau+1)/2)}{\eta((\tau+1)/2)} - 8\frac{\eta'(2\tau)}{\eta(2\tau)}\right], \\
Y_2(\tau) &= \frac{\sqrt{3}i}{4\pi}\left[\frac{\eta'(\tau/2)}{\eta(\tau/2)} - \frac{\eta'((\tau+1)/2)}{\eta((\tau+1)/2)}\right],
\end{aligned} \tag{A21}$$

Furthermore, $\eta(\tau)$ is the Dedekind function which is defined as follows:

$$\eta(\tau) = q^{1/24} \prod_{n=1}^{\infty} (1-q^n)\,, \qquad q \equiv e^{2\pi i \tau}\,. \tag{A22}$$

Then, the modular forms $Y_{1,2}(\tau)$ can be expressed as follows [45]:

$$\begin{aligned} Y_1(\tau) &= 1/8 + 3q + 3q^2 + 12q^3 + 3q^4 + 18q^5 + 12q^6 + 24q^7 + 3q^8 + 39q^9 + 18q^{10}\cdots\,, \\ Y_2(\tau) &= \sqrt{3}q^{1/2}(1 + 4q + 6q^2 + 8q^3 + 13q^4 + 12q^5 + 14q^6 + 24q^7 + 18q^8 + 20q^9\cdots). \end{aligned} \tag{A23}$$

The modular multiplets of level $N = 2$ up to weight 8 are given by:

$$\begin{aligned}
&Y^{(4)}_{\mathbf{1}} = \left(Y^{(2)}_{\mathbf{2}} Y^{(2)}_{\mathbf{2}}\right)_{\mathbf{1}} = (Y^{(2)}_{\mathbf{2},1})^2 + (Y^{(2)}_{\mathbf{2},2})^2\,, && Y^{(4)}_{\mathbf{2}} = \left(Y^{(2)}_{\mathbf{2}} Y^{(2)}_{\mathbf{2}}\right)_{\mathbf{2}} = \begin{pmatrix} (Y^{(2)}_{\mathbf{2},2})^2 - (Y^{(2)}_{\mathbf{2},1})^2 \\ 2Y^{(2)}_{\mathbf{2},1} Y^{(2)}_{\mathbf{2},2} \end{pmatrix}, \\
&Y^{(6)}_{\mathbf{1}} = \left(Y^{(2)}_{\mathbf{2}} Y^{(4)}_{\mathbf{2}}\right)_{\mathbf{1}} = Y^{(2)}_{\mathbf{2},1} Y^{(4)}_{\mathbf{2},1} + Y^{(2)}_{\mathbf{2},2} Y^{(4)}_{\mathbf{2},2}\,, && Y^{(6)}_{\mathbf{1'}} = \left(Y^{(2)}_{\mathbf{2}} Y^{(4)}_{\mathbf{2}}\right)_{\mathbf{1'}} = Y^{(2)}_{\mathbf{2},1} Y^{(4)}_{\mathbf{2},2} - Y^{(2)}_{\mathbf{2},2} Y^{(4)}_{\mathbf{2},1}\,, \\
&Y^{(6)}_{\mathbf{2}} = \left(Y^{(2)}_{\mathbf{2}} Y^{(4)}_{\mathbf{1}}\right)_{\mathbf{2}} = \begin{pmatrix} Y^{(2)}_{\mathbf{2},1} Y^{(4)}_{\mathbf{1}} \\ Y^{(2)}_{\mathbf{2},2} Y^{(4)}_{\mathbf{1}} \end{pmatrix}, && Y^{(8)}_{\mathbf{1}} = \left(Y^{(4)}_{\mathbf{1}} Y^{(4)}_{\mathbf{1}}\right)_{\mathbf{1}} = (Y^{(4)}_{\mathbf{1}})^2\,, \\
&Y^{(8)}_{\mathbf{2a}} = \left(Y^{(4)}_{\mathbf{1}} Y^{(4)}_{\mathbf{2}}\right)_{\mathbf{2}} = \begin{pmatrix} Y^{(4)}_{\mathbf{1}} Y^{(4)}_{\mathbf{2},1} \\ Y^{(4)}_{\mathbf{1}} Y^{(4)}_{\mathbf{2},2} \end{pmatrix}, && Y^{(8)}_{\mathbf{2b}} = \left(Y^{(4)}_{\mathbf{2}} Y^{(4)}_{\mathbf{2}}\right)_{\mathbf{2}} = \begin{pmatrix} (Y^{(4)}_{\mathbf{2},2})^2 - (Y^{(4)}_{\mathbf{2},1})^2 \\ 2Y^{(4)}_{\mathbf{2},1} Y^{(4)}_{\mathbf{2},2} \end{pmatrix}.
\end{aligned} \tag{A24}$$

---

[1] F. Feruglio, *Are neutrino masses modular forms?*, pp. 227–266. 2019. arXiv:1706.08749 [hep-ph].

[2] G.-J. Ding and S. F. King, "Neutrino mass and mixing with modular symmetry," *Rept. Prog. Phys.* **87** no. 8, (2024) 084201, arXiv:2311.09282 [hep-ph].

[3] P. P. Novichkov, J. T. Penedo, S. T. Petcov, and A. V. Titov, "Modular A_5 symmetry for flavour model building," *JHEP* **04** (2019) 174, arXiv:1812.02158 [hep-ph].

[4] S. F. King and Y.-L. Zhou, "Trimaximal TM_1 mixing with two modular S_4 groups," *Phys. Rev. D* **101** no. 1, (2020) 015001, arXiv:1908.02770 [hep-ph].

[5] H. Okada and Y. Orikasa, "Modular S_3 symmetric radiative seesaw model," *Phys. Rev. D* **100** no. 11, (2019) 115037, arXiv:1907.04716 [hep-ph].

[6] X.-G. Liu and G.-J. Ding, "Neutrino Masses and Mixing from Double Covering of Finite Modular Groups," *JHEP* **08** (2019) 134, arXiv:1907.01488 [hep-ph].

[7] T. Kobayashi, Y. Shimizu, K. Takagi, M. Tanimoto, and T. H. Tatsuishi, "Modular S_3-invariant flavor model in SU(5) grand unified theory," *PTEP* **2020** no. 5, (2020) 053B05, arXiv:1906.10341 [hep-ph].

[8] X. Du and F. Wang, "SUSY breaking constraints on modular flavor S_3 invariant SU(5) GUT model," *JHEP* **02** (2021) 221, arXiv:2012.01397 [hep-ph].

[9] M. Abbas, "Fermion masses and mixing in modular A4 Symmetry," *Phys. Rev. D* **103** no. 5, (2021) 056016, arXiv:2002.01929 [hep-ph].

[10] P. P. Novichkov, J. T. Penedo, and S. T. Petcov, "Fermion mass hierarchies, large lepton mixing and residual modular symmetries," *JHEP* **04** (2021) 206, arXiv:2102.07488 [hep-ph].

[11] K. Ishiguro, H. Okada, and H. Otsuka, "Residual flavor symmetry breaking in the landscape of modular flavor models," *JHEP* **09** (2022) 072, arXiv:2206.04313 [hep-ph].

[12] M.-C. Chen, S. F. King, O. Medina, and J. W. F. Valle, "Quark-lepton mass relations from modular flavor symmetry," *JHEP* **02** (2024) 160, arXiv:2312.09255 [hep-ph].

[13] D. Meloni and M. Parriciatu, "A simplest modular S_3 model for leptons," *JHEP* **09** (2023) 043, arXiv:2306.09028 [hep-ph].

[14] T. Kobayashi, T. Nomura, H. Okada, and H. Otsuka, "Modular flavor models with positive modular weights: a new lepton model building," *JHEP* **01** (2024) 121, arXiv:2310.10091 [hep-ph].

[15] G.-J. Ding, S.-Y. Jiang, S. F. King, J.-N. Lu, and B.-Y. Qu, "Pati-Salam models with A_4 modular symmetry," *JHEP* **08** (2024) 134, arXiv:2404.06520 [hep-ph].

[16] M. Belfkir, M. A. Loualidi, and S. Nasri, "Fermion Masses and Mixing in Pati-Salam Unification with S_3 Modular Symmetry," arXiv:2501.00302 [hep-ph].

[17] S. Marciano, D. Meloni, and M. Parriciatu, "Minimal seesaw and leptogenesis with the smallest modular finite group," *JHEP* **05** (2024) 020, arXiv:2402.18547 [hep-ph].

[18] S. J. D. King and S. F. King, "Fermion mass hierarchies from modular symmetry," *JHEP* **09** (2020) 043, arXiv:2002.00969 [hep-ph].

[19] P. Minkowski, "$\mu \to e\gamma$ at a Rate of One Out of 10^9 Muon Decays?," *Phys. Lett. B* **67** (1977) 421–428.

[20] T. Yanagida, "Horizontal gauge symmetry and masses of neutrinos," *Conf. Proc. C* **7902131** (1979) 95–99.

[21] M. Gell-Mann, P. Ramond, and R. Slansky, "Complex Spinors and Unified Theories," *Conf. Proc. C* **790927** (1979) 315–321, arXiv:1306.4669 [hep-th].

[22] S. L. Glashow, "The Future of Elementary Particle Physics," *NATO Sci. Ser. B* **61** (1980) 687.

[23] R. N. Mohapatra and G. Senjanovic, "Neutrino Mass and Spontaneous Parity Nonconservation," *Phys. Rev. Lett.* **44** (1980) 912.

[24] J. Schechter and J. W. F. Valle, "Neutrino Masses in SU(2) x U(1) Theories," *Phys. Rev. D* **22** (1980) 2227.

[25] J. C. Pati and A. Salam, "Lepton Number as the Fourth Color," *Phys. Rev. D* **10** (1974) 275–289. [Erratum: Phys.Rev.D 11, 703–703 (1975)].

[26] C. D. Froggatt and H. B. Nielsen, "Hierarchy of Quark Masses, Cabibbo Angles and CP Violation," *Nucl. Phys. B* **147** (1979) 277–298.

[27] Z. G. Berezhiani, "The Weak Mixing Angles in Gauge Models with Horizontal Symmetry: A New Approach to Quark and Lepton Masses," *Phys. Lett. B* **129** (1983) 99–102.

[28] S. Rajpoot, "See-saw masses for quarks and leptons in an ambidextrous electroweak interaction model," *Mod. Phys. Lett. A* **2** no. 5, (1987) 307–315. [Erratum: Mod.Phys.Lett.A 2, 541 (1987)].

[29] A. Davidson and K. C. Wali, "Universal Seesaw Mechanism?," *Phys. Rev. Lett.* **59** (1987) 393.

[30] A. Davidson and K. C. Wali, "SU(5)-L x SU(5)-R HYBRID UNIFICATION," *Phys. Rev. Lett.* **58** (1987) 2623.

[31] G. Valencia and S. Willenbrock, "Quark - lepton unification and rare meson decays," *Phys. Rev. D* **50** (1994) 6843–6848, arXiv:hep-ph/9409201.

[32] A. D. Smirnov, "Mass limits for scalar and gauge leptoquarks from K(L)0 —> e-+ mu+-, B0 —> e-+ tau+- decays," *Mod. Phys. Lett. A* **22** (2007) 2353–2363, arXiv:0705.0308 [hep-ph].

[33] R. N. Mohapatra, "Mechanism for Understanding Small Neutrino Mass in Superstring Theories," *Phys. Rev. Lett.* **56** (1986) 561–563.

[34] S. F. King, *Right-handed neutrinos: seesaw models and signatures*. 2, 2025. arXiv:2502.07877 [hep-ph].

[35] Z.-z. Xing, "Flavor structures of charged fermions and massive neutrinos," *Phys. Rept.* **854** (2020) 1–147, arXiv:1909.09610 [hep-ph].

[36] **Particle Data Group** Collaboration, R. Workman *et al.*, "Review of Particle Physics," *PTEP* **2022** (2022) 083C01.

[37] P. F. de Salas, D. V. Forero, S. Gariazzo, P. Martínez-Miravé, O. Mena, C. A. Ternes, M. Tórtola, and J. W. F. Valle, "2020 global reassessment of the neutrino oscillation picture," *JHEP* **02** (2021) 071, arXiv:2006.11237 [hep-ph].

[38] I. Esteban, M. C. Gonzalez-Garcia, M. Maltoni, I. Martinez-Soler, J. a. P. Pinheiro, and T. Schwetz, "NuFit-6.0: Updated global analysis of three-flavor neutrino oscillations," arXiv:2410.05380 [hep-ph].

[39] **Planck** Collaboration, N. Aghanim *et al.*, "Planck 2018 results. VI. Cosmological parameters," *Astron. Astrophys.* **641** (2020) A6, arXiv:1807.06209 [astro-ph.CO]. [Erratum: Astron.Astrophys. 652, C4 (2021)].

[40] **KamLAND-Zen** Collaboration, S. Abe *et al.*, "Search for the Majorana Nature of Neutrinos in the Inverted Mass Ordering Region with KamLAND-Zen," *Phys. Rev. Lett.* **130** no. 5, (2023) 051801, arXiv:2203.02139 [hep-ex].

[41] **nEXO** Collaboration, G. Adhikari *et al.*, "nEXO: neutrinoless double beta decay search beyond 10^{28} year half-life sensitivity," *J. Phys. G* **49** no. 1, (2022) 015104, arXiv:2106.16243 [nucl-ex].

[42] R. de Adelhart Toorop, F. Feruglio, and C. Hagedorn, "Finite Modular Groups and Lepton Mixing," *Nucl. Phys. B* **858** (2012) 437–467, arXiv:1112.1340 [hep-ph].

[43] H. Ishimori, T. Kobayashi, H. Ohki, Y. Shimizu, H. Okada, and M. Tanimoto, "Non-Abelian Discrete Symmetries in Particle Physics," *Prog. Theor. Phys. Suppl.* **183** (2010) 1–163, arXiv:1003.3552 [hep-th].

[44] T. Kobayashi, K. Tanaka, and T. H. Tatsuishi, "Neutrino mixing from finite modular groups," *Phys. Rev. D* **98** no. 1, (2018) 016004, arXiv:1803.10391 [hep-ph].

[45] C.-C. Li and G.-J. Ding, "Eclectic flavor group $\Delta(27) \rtimes S_3$ and lepton model building," *JHEP* **03** (2024) 054, arXiv:2308.16901 [hep-ph].